

Time invariant property of weighted circular convolution and its application to continuous wavelet transform

Hua Yi^{*}, Yu-Le RU, and Yin-Yun DAI

School of Mathematics and Physics, Jinggangshan University, Ji'an, 343009, P.R. China

Abstract. Time invariant linear operators are the building blocks of signal processing. Weighted circular convolution and signal processing framework in a generalized Fourier domain are introduced by Jorge Martinez. In this paper, we prove that under this new signal processing framework, weighted circular convolution also has a generalized time invariant property. We also give an application of this property to algorithm of continuous wavelet transform (CWT). Specifically, we have previously studied the algorithm of CWT based on generalized Fourier transform with parameter 1. In this paper, we prove that the parameter can take any complex number. Numerical experiments are presented to further demonstrate our analyses.

Key words: continuous wavelet transform; linear convolution; weighted circular convolution; generalized discrete Fourier transform.

1. INTRODUCTION

Nowadays, wavelets are a powerful tool which has been used in numerical techniques [1–3]. Wavelets theory are mostly used in the areas of applied engineering and sciences [4–6]. Specifically, wavelet transform can provide time-frequency localization analysis [7]. There is no position (or time) information in frequency analysis provided by Fourier transform [8]. An example of signal analysis by wavelet transform and Fourier transform is given in Fig. 1 [9]. Another example of signal analysis of climate data by wavelet transform is given in Fig. 2 [10].

Time invariant linear operators, such as linear convolution and circular convolution, play an important role in classic discrete signal processing algorithms [11, 12]. Circular convolution has a FFT-based fast algorithm due to convolution theorem [13]. Linear convolution is usually calculated by applying circular convolution on signals doubled with zero-padding [13, 14]. Right angle circular convolution [15], skew-cyclic convolution [16] weighted circular convolution [17] etc. are also introduced to study the computation of linear convolution.

Linear time invariant operators can be used in the algorithm design of continuous wavelet transform (CWT) [18, 19]. CWT is a linear convolution of signal and wavelet function for a fixed scale [9]. In general, the time domain sampling of wavelet function has the following form [12]

$$p = (h(-aT), h(-aT + 1), \dots, h(-1), h(0), h(1), \dots, h(aT), 0, \dots, 0). \quad (1)$$

If the CWT is computed directly by the linear convolution of signal and p , then this method is known as time-domain algorithm of CWT [12]. The discrete Fourier transform (DFT) of p is

$$\text{DFT}_p \approx e^{-iaT\omega} \hat{\psi}^*(a\omega) \Big|_{\omega = \left[\frac{2\pi \cdot 0}{N}, \frac{2\pi \cdot 1}{N}, \dots, \frac{2\pi \cdot (N-1)}{N} \right]^T}, \quad (2)$$

where ψ is the analytic expression of mother wavelet. By considering the shift property of DFT and (2). It is natural to define a filter q such that [12]

$$\text{DFT}_q \approx \hat{\psi}^*(a\omega) \Big|_{\omega = \left[\frac{2\pi \cdot 0}{N}, \frac{2\pi \cdot 1}{N}, \dots, \frac{2\pi \cdot (N-1)}{N} \right]^T}. \quad (3)$$

By the shift property of DFT, (2) and (3), we know that [12]

$$R_{aT}q = p. \quad (4)$$

So the convolution of signal x and p can be transformed into the convolution of signal and q . According to the time invariant property of convolution, we have

$$x \star p = x \star R_{aT}q = R_{aT}(x \star q), \quad (5)$$

where \star can be linear convolution or circular convolution.

The method using $R_{aT}(x \star q)$ to compute CWT is known as frequency-domain algorithm of CWT [12].

One of the main tasks of this paper is to study the time invariant properties of weighted circular convolution which is a generalization of (5). We need to study it in the generalized Fourier domain (GFD). For a finite-length signal, weighted periodic signal extension will naturally occur when working in GFD [17, 20]. In fact, the signal is weighted periodic in time domain and periodic in GFD.

The definition of generalized discrete Fourier transform (GDFT) of causal signal and that of non causal signal are introduced in Ref. [17] and Ref. [12] respectively. If p defined

*e-mail: 876145777@qq.com

Manuscript submitted 2020-10-26, revised 2021-06-03, initially accepted for publication 2021-06-09, published in August 2021

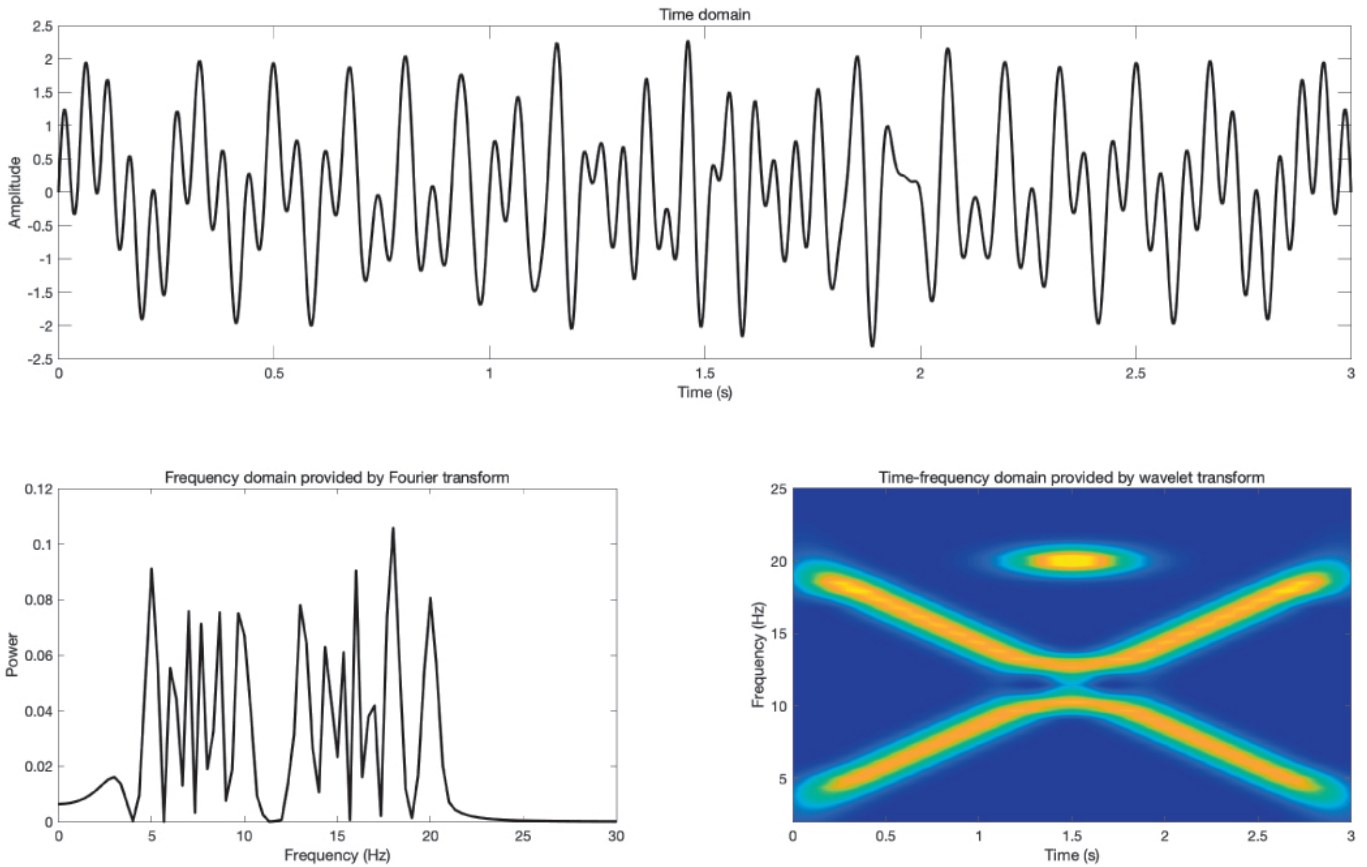


Fig. 1. This figure is the figure 1 in [9]. This figure shows that wavelet transform can provide time-frequency localization analysis. There is no position information in time-frequency analysis provided by Fourier transform

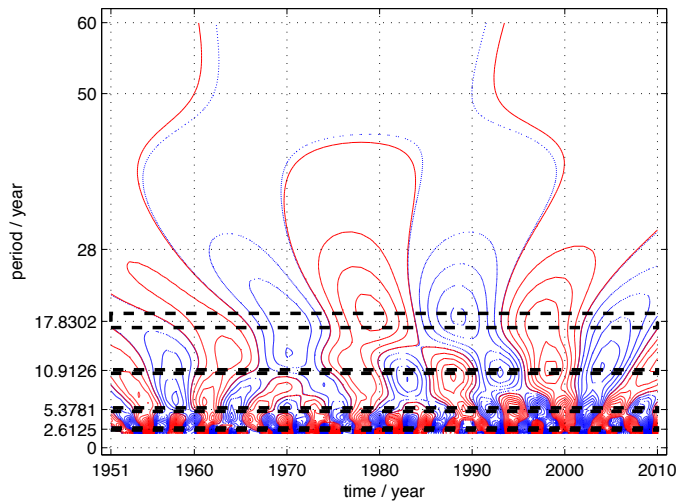


Fig. 2. This figure is the figure 10 in [10]. This figure shows the contour of the real part of wavelet transform of the monthly average temperature of No. 50978 from January 1, 1951 to December 31, 2010

in (1) is regarded as a non causal signal and the definition of GDFT of non causal signal is adopted, then GDFT of p is [12]

$$(\mathcal{F}_\alpha p)(k) \approx e^{-\frac{iaT2\pi k}{N}} \hat{\psi}^* \left(a \left(\frac{2\pi k}{N} + i\beta \right) \right), \quad \text{for } k = 0, 1, \dots, N-1. \quad (6)$$

By considering the relationship between (2) and (3), according to (6), we hope to find a q such that

$$(\mathcal{F}_\alpha q)(k) \approx \hat{\psi}^* \left(a \left(\frac{2\pi k}{N} + i\beta \right) \right), \quad \text{for } k = 0, 1, \dots, N-1. \quad (7)$$

Surprisingly, q satisfying (7) is exactly [12]

$$R_{aT} q = p, \quad (8)$$

where R_k is a weighted circular shift operator, and R_k defined in (4) a circular shift operator. To simplify the notation, the same symbol here represents different meanings. The reader should be able to understand the meaning according to the context.

Weighted circular convolution has also been used to study the algorithm of CWT since CWT is a linear convolution of signal and wavelet function for a fixed scale [12]. The method using the weighted circular convolution of signal and q (see equation (35)) to compute CWT is known as GDFT-based algorithm of CWT [12].

In this paper, time invariant properties of weighted circular convolution are used to deduce the algorithm of CWT. Some new results are obtained in this paper, which generalizes the previous results of Ref. [12]. Specifically, Ref. [12] only considers GDFT-based algorithm for CWT with parameter $\alpha = 1$, but in this paper, we can consider the algorithm with parame-

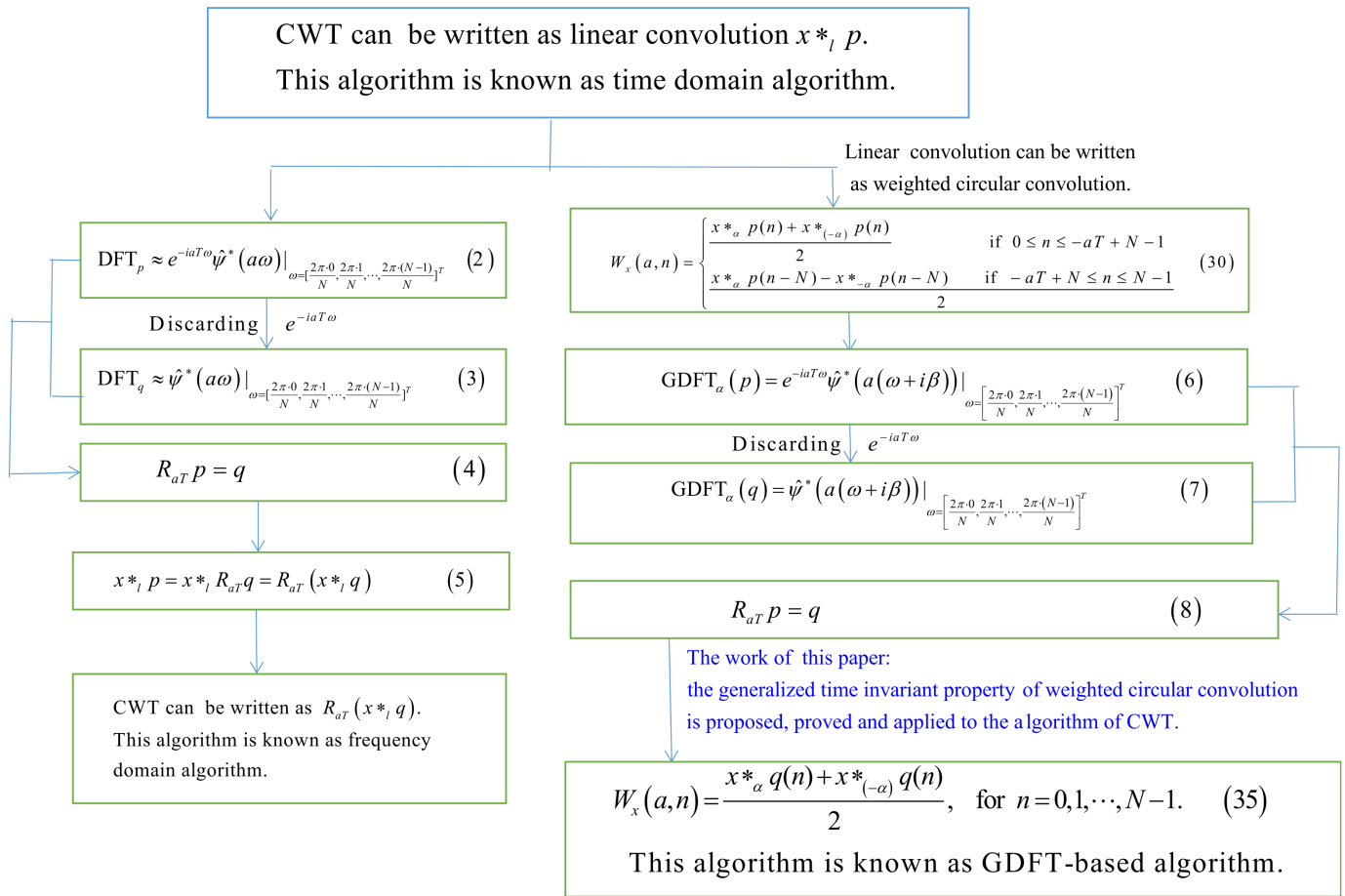


Fig. 3. Block diagram shows the research framework and innovation of this paper

ter of arbitrary complex number. Figure 3 shows the research framework and innovation of this paper.

This paper is organized as follows. In section 2, the definitions of GDFT and inverse GDFT are given firstly. Then time domain shift property of GDFT is deduced. In section 3, we firstly give the mutual representation of linear convolution and weighted circular convolution. Secondly, the fast algorithm of weighted circular convolution is presented. Lastly, time invariant properties of weighted circular convolution are derived. In section 4, the theory and algorithms of CWT are studied. Section 5 presents numerical experiments to demonstrate our analyses and finally, We end this paper with conclusions in section 6.

2. GDFT AND ITS PROPERTIES

Definition 1. Let us define the generalized discrete Fourier transform (GDFT) for finite-length signal

$$h = \left\{ h(n) \right\}_{n=-M}^{-M+N-1}, \quad (9)$$

where $0 \leq M < N$, with parameter $\alpha \in C \setminus \{0\}$ as

$$(\mathcal{F}_\alpha h)(k) \stackrel{\text{def}}{=} H_\alpha(k) = \sum_{n=-M}^{-M+N-1} h(n) e^{\beta n} e^{-i(2\pi/N)k(n+M)}, \quad (10)$$

for $k = 0, 1, \dots, N-1,$

where $\beta = \log(\alpha)/N$. The inverse GDFT is given by,

$$(\mathcal{F}_\alpha^{-1}H_\alpha)(n) \stackrel{\text{def}}{=} h(n) = \frac{e^{-\beta n}}{N} \sum_{k=0}^{N-1} H_\alpha(k) e^{i(2\pi/N)k(n+M)},$$

for $n = -M, -M+1, \dots, -M+N-1$. (11)

If $M = 0$ in (10) and (11), the definitions of GDFT and the inverse GDFT are the same as that of Refs. [17, 20].

From (10), we know that $\mathcal{F}_\alpha h$ is periodic with period N . From (11), we have $\{h(n)\}_{n \in \mathbb{Z}}$ which is a weighted periodic extension [17, 20] of $\{h(n)\}_{n=-M, -M+1, \dots, -M+N-1}$. Particularly, we have

$$h(-M : N-1) = (h(-M), h(-M+1), \dots, h(-1), h(0), \dots, h(-M+N-1), \frac{1}{\alpha}h(-M), \frac{1}{\alpha}h(-M+1), \dots, \frac{1}{\alpha}h(-1)). \quad (12)$$

In fact, if $n \in [-M+N, N-1]$, thus $n' = n - N \in [-M, -1]$. From (11), we have

$$\begin{aligned} h(n) &= \frac{e^{-\beta n}}{N} \sum_{k=0}^{N-1} H_\alpha[k] e^{i(2\pi/N)k(n+M)} \\ &= \frac{e^{-\beta(n'+N)}}{N} \sum_{k=0}^{N-1} H_\alpha[k] e^{i(2\pi/N)k(n'+M+N)} \\ &= \frac{1}{e^{\beta N}} \frac{e^{-\beta n'}}{N} \sum_{k=0}^{N-1} H_\alpha[k] e^{i(2\pi/N)k(n'+M)} \\ &= \frac{1}{\alpha} h(n-N). \end{aligned}$$

Thus, (12) is obtained. For the clarity of notation, we denote

$$\begin{aligned} p(-M : -M+N-1) &\stackrel{\text{def}}{=} h(-M : -M+N-1) \\ &= (h(-M), h(-M+1), \dots, h(-1), h(0), \dots, h(-M+N-1)); \\ q(0 : N-1) &\stackrel{\text{def}}{=} h(0 : N-1) = (h(0), \dots, h(-M+N-1), \\ &\quad \frac{1}{\alpha}h(-M), \frac{1}{\alpha}h(-M+1), \dots, \frac{1}{\alpha}h(-1)). \end{aligned} \quad (13)$$

From (13), we see that both p, q are different parts of $\{h(n)\}_{n \in \mathbb{Z}}$, where the domains of definition of p and q are $\{-M, -M+1, \dots, -M+N-1\}$ and $\{0, 1, \dots, N-1\}$ respectively.

Define weighted circular shift operator as

$$(R_k h)(n) = h(n-k), \quad \text{for } n \in \mathbb{Z}. \quad (14)$$

It should be noted that R_k only has practical significance for finite length signals. For example, from (5), we know that R_k acts on the finite length signal q or $x \star q$.

Writing p and q in (13) together, we have

$$\begin{aligned} p &= (p(-M), \dots, p(-1), p(0), \dots, p(-M+N-1)), \\ q &= \left(p(0), \dots, p(-M+N-1), \frac{p(-M)}{\alpha}, \dots, \frac{p(-1)}{\alpha} \right). \end{aligned} \quad (15)$$

From (15), we see that

$$R_M q = p, \quad (16)$$

and R_M is a right shift by M .

Next, we present the shift property [21] for the GDFT. It should be noted that this shift property in this paper is different from that of Ref. [20] because the definition of GDFT for non causal signal in Ref. [20] is different from that of this paper.

Proposition 1. time domain shift property of GDFT: Suppose q and $R_M q$ is defined in (13) and (16). Then

$$(\mathcal{F}_\alpha \{R_M q\})(k) = e^{-i(2\pi/N)kM} (\mathcal{F}_\alpha q)(k), \quad k = 0, 1, \dots, N-1, \quad (17)$$

Proof. By equations (10), (13) and (16), we have

$$\begin{aligned} (\mathcal{F}_\alpha \{R_M q\})(k) &= (\mathcal{F}_\alpha p)(k) \\ &= \sum_{n=-M}^{-M+N-1} h(n) e^{\beta n} e^{-i(2\pi/N)k(n+M)} \\ &= e^{-i(2\pi/N)kM} \left(\sum_{n=-M}^{-1} h(n) e^{\beta n} e^{-i(2\pi/N)kn} \right. \\ &\quad \left. + \sum_{n=0}^{-M+N-1} h(n) e^{\beta n} e^{-i(2\pi/N)kn} \right) \\ &= e^{-i(2\pi/N)kM} \left(\sum_{n=-M}^{-1} \frac{1}{\alpha} h(n) e^{\beta(n+N)} e^{-i(2\pi/N)kn} \right. \\ &\quad \left. + \sum_{n=0}^{-M+N-1} h(n) e^{\beta n} e^{-i(2\pi/N)kn} \right) \\ &= e^{-i(2\pi/N)kM} \left(\sum_{n=-M}^{-1} h(n+N) e^{\beta(n+N)} e^{-i(2\pi/N)k(n+N)} \right. \\ &\quad \left. + \sum_{n=0}^{-M+N-1} h(n) e^{\beta n} e^{-i(2\pi/N)kn} \right) \\ &= e^{-i(2\pi/N)kM} (\mathcal{F}_\alpha q)(k), \quad \text{for } k = 0, 1, \dots, N-1. \end{aligned}$$

3. LINEAR CONVOLUTION AND WEIGHTED CIRCULAR CONVOLUTION

Let $x = \{x(n)\}_{n=0}^{N-1}$, $X_\alpha = \mathcal{F}_\alpha x$. Let $P_\alpha = \mathcal{F}_\alpha p$, $Q_\alpha = \mathcal{F}_\alpha q$, where p, q are defined in (13). Let $\star_\ell, \star_c, \star_\alpha$ represent linear convolution, circular convolution, weighted circular convolution with parameter α , respectively.

3.1. The relationship of linear convolution and weighted circular convolution

The linear convolution of $x = \{x(n)\}_{n=0}^{N-1}$ and $p = \{p(n)\}_{n=-M}^{-M+N-1}$ can be expressed as [12]

$$\begin{bmatrix} x \star_\ell p(-M) \\ x \star_\ell p(-M+1) \\ \vdots \\ x \star_\ell p(-M+2N-2) \end{bmatrix} = P \cdot \begin{bmatrix} x(0) \\ x(1) \\ \vdots \\ x(N-1) \end{bmatrix},$$

3.3. Time-invariant property of weighted circular convolution

Time invariant property of circular convolution has been proved in Ref. [12], namely

$$x \star_c (R_M q) = R_M (x \star_c q). \quad (25)$$

This property has been used to deduce the frequency domain algorithm of CWT [12]. For the signal processing framework based on Fourier domain and generalized Fourier domain, the discretization of time domain signal will lead to the period of frequency domain signal. Therefore, the proof idea of (26) is the same as that of (25). It should be noted that the operator R_M in (25) represents circular shift, while the operator R_M in (26) represents weighted circular shift [12].

Theorem 1. Time-invariant property of weighted circular convolution:

$$x \star_\alpha (R_M q) = R_M (x \star_\alpha q). \quad (26)$$

Proof. It is easy to check that the definition domain of $x \star_\alpha (R_M q)$ and $R_M (x \star_\alpha q)$ are the same, namely, $\{-M, -M+1, \dots, -M+N-1\}$. It suffices to show that the two signals have a common generalized frequency domain representation. By (22) and (17),

$$\begin{aligned} (\mathcal{F}_\alpha(x \star_\alpha (R_M q)))(k) &= \\ (\mathcal{F}_\alpha x)(k) \mathcal{F}_\alpha (R_M q)(k) &= (\mathcal{F}_\alpha x)(k) (\mathcal{F}_\alpha q)(k) e^{-\frac{2\pi i k M}{N}}; \\ (\mathcal{F}_\alpha \{R_M (x \star_\alpha q)\})(k) &= (\mathcal{F}_\alpha x)(k) (\mathcal{F}_\alpha q)(k) e^{-\frac{2\pi i k M}{N}}, \\ &\text{for } k = 0, 1, \dots, N-1. \end{aligned}$$

Thus

$$\mathcal{F}_\alpha \{x \star_\alpha (R_M q)\} = \mathcal{F}_\alpha \{R_M (x \star_\alpha q)\}.$$

□

Corollary 1.

$$x \star_\alpha q(n) = \begin{cases} x \star_\alpha p(n) & \text{if } n \in \{0, 1, \dots, -M+N-1\} \\ \frac{x \star_\alpha p(n-N)}{\alpha} & \text{if } n \in \{N-M, N-M+1, \dots, N-1\} \end{cases}. \quad (27)$$

Proof. From (16) and (26), we have

$$x \star_\alpha p = x \star_\alpha (R_M q) = R_M (x \star_\alpha q).$$

By noting that R_M represents weighted circular shift operator and repeating the derivation process of (12), (27) is obtained. □

4. APPLICATION: THE ALGORITHM OF CWT AND NUMERICAL EXPERIMENTS

Assume that the support of the mother wavelet $\psi(t)$ is $[-T, T]$. The discrete version of continuous wavelet transform of a signal $\{x(k)\}_{k=0}^{N-1}$ at a scale $a \in R^+$ with this mother wavelet is expressed by the following linear convolution [12]

$$W_x(a, n) = x \star_\ell p(n), n = 0, 1, \dots, N-1, \quad (28)$$

where

$$p(-aT : -aT + N - 1) = (h(-aT), h(-aT + 1), \dots, h(-1), h(0), \dots, h(aT), 0, \dots, 0), \quad (29)$$

and

$$h(k) = \frac{1}{a} \Psi^* \left(\frac{-k}{a} \right), \quad \text{for } k = -aT, -aT+1, \dots, aT.$$

By (21), the linear convolution in (28) can be represented as weighted circular convolution,

$$W_x(a, n) = \begin{cases} \frac{x \star_\alpha p(n) + x \star_{(-\alpha)} p(n)}{2}, & \text{if } 0 \leq n \leq -aT + N - 1, \\ \frac{x \star_\alpha p(n-N) - x \star_{(-\alpha)} p(n-N)}{2\alpha}, & \text{if } -aT + N \leq n \leq N - 1. \end{cases} \quad (30)$$

The weighted periodic extension of (29) is

$$h(-aT : N - 1) = (h(-aT), h(-aT + 1), \dots, h(-1), h(0), \dots, h(aT), 0, \dots, 0, \frac{1}{\alpha} h(-aT), \frac{1}{\alpha} h(-aT + 1), \dots, \frac{1}{\alpha} h(-1)). \quad (31)$$

Define

$$q(0 : N - 1) = h(0 : N - 1). \quad (32)$$

Then

$$R_{aT} q = p. \quad (33)$$

Lemma 1.

$$\frac{x \star_\alpha q(n) + x \star_{(-\alpha)} q(n)}{2} = \begin{cases} \frac{x \star_\alpha p(n) + x \star_{(-\alpha)} p(n)}{2}, & \text{if } 0 \leq n \leq -aT + N - 1, \\ \frac{x \star_\alpha p(n-N) - x \star_{(-\alpha)} p(n-N)}{2\alpha}, & \text{if } -aT + N \leq n \leq N - 1. \end{cases} \quad (34)$$

Proof. By corollary 1, if $0 \leq n \leq -aT + N - 1$, then $x \star_\alpha q(n) = x \star_\alpha p(n)$ and $x \star_{(-\alpha)} q(n) = x \star_{(-\alpha)} p(n)$. Thus the first part of (34) is proved. If $-aT + N \leq n \leq N - 1$, then $x \star_\alpha q(n) = \frac{x \star_\alpha p(n-N)}{\alpha}$ and $x \star_{(-\alpha)} q(n) = \frac{x \star_{(-\alpha)} p(n-N)}{-\alpha}$ by corollary 1. Thus the last part of (34) can be proved. □

Theorem 2.

$$W_x(a, n) = \frac{x \star_\alpha q(n) + x \star_{(-\alpha)} q(n)}{2}, \quad \text{for } n = 0, 1, \dots, N-1, \quad (35)$$

where $\alpha \in C \setminus \{0\}$.

Proof. By (30) and (34), (35) can be obtained. □

Corollary 2. [12] If $\alpha = 1$ in theorem 2, then

$$W_x(a, n) = \frac{x \star_1 q(n) + x \star_{(-1)} q(n)}{2},$$

for $n = 0, 1, \dots, N-1$. (36)

Only $\alpha = 1$ is considered in GDFT based algorithm for the computation of CWT in Ref. [12]. However, In this paper, any $\alpha \in C$ may be used.

Algorithm 1. GDFT based algorithm for CWT

Input:

the signal, $f[n], n = 0, 1, \dots, N-1$

scale, a

parameter, $\alpha \in C$

$\hat{\psi}(\omega)$, the Fourier transform of the Morlet wavelet $\psi(t)$

Output:

wavelet coefficients, $W_f^a[i], i = 0, 1, \dots, N-1$

1. Let $f = [f_0, f_1, \dots, f_{N-1}]^T$;
2. for $\gamma = [\alpha, -\alpha]$;
3. Let $\beta = \frac{\log \gamma}{N}$;
4. Let $\mathcal{F}_\gamma q = \hat{\psi}^*(a(\frac{2\pi k}{N} + i\beta))|_{k=[0,1,\dots,N-1]^T}$;
5. $z_\gamma[i] = \mathcal{F}_\gamma^{-1}(\mathcal{F}_\gamma f * \mathcal{F}_\gamma q), i = 0, 1, \dots, N-1$.
6. end for
7. $W_f^a[i] = \frac{z_\alpha[i] + z_{-\alpha}[i]}{2}, i = 0, 1, \dots, N-1$.

5. NUMERICAL EXPERIMENTS

We will repeat experiments previously done in Ref. [12], with various algorithms. Specifically, GDFT-based algorithm with parameter $\alpha = 1$ is considered in Ref. [12]. However, in this paper, any $\alpha \in C$ may be used.

For the signal with length $n = 1024$ in Fig. 1 of Ref. [12], we conduct Morlet wavelet transform, where the Morlet wavelet parameters are $\sigma^2 = 1, \eta = 5$, using various algorithms.

The various algorithms are time domain algorithm [12, 23], frequency domain algorithm [12, 23], GDFT based algorithm with parameters $\alpha = 1, 3, 5, \dots, 19, i, 3i, 5i, \dots, 19i, 1+i, 3+3i, 5+5i, \dots, 19+19i, 38+38i, 380+380i, 3800+3800i, 38000+38000i$.

The mean squared errors $\left(MSE = \frac{1}{n} \sum_{i=1}^n (Y_i - \hat{Y}_i)^2 \right)$ of wavelet coefficients of various algorithms compared with GDFT based algorithm($\alpha = 1$) are shown in Table 1.

Table 2 is the same with Table 1, but the Morlet wavelet parameters are $\sigma^2 = 1, \eta = 6$.

From Table 1 and 2, some information can be drawn.

- If the modulus of the parameter α is not too large, the errors among the algorithms based on GDFT with different parameter α is small. This shows that these algorithms have a closer relationship.
- The error between GDFT based algorithm($\alpha = 1$) and frequency-domain algorithm is less than that between GDFT based algorithm($\alpha = 1$) and time-domain algorithm. This shows that the relationship between GDFT based algorithm($\alpha = 1$) and frequency-domain algorithm is closer than that between GDFT based algorithm($\alpha = 1$) and time-domain algorithm.

Table 1

The mean squared errors ($MSE = \frac{1}{n} \sum_{i=1}^n (Y_i - \hat{Y}_i)^2$) of wavelet coefficients of various algorithms compared with GDFT based algorithm($\alpha = 1$). The Morlet wavelet parameters are $\sigma^2 = 1, \eta = 5$. The various algorithms are time domain algorithm [12, 23], frequency domain algorithm [12, 23], GDFT based algorithm with parameters $\alpha = 1, 3, 5, \dots, 19, i, 3i, 5i, \dots, 19i, 1+i, 3+3i, 5+5i, \dots, 19+19i, 38+38i, 380+380i, 3800+3800i, 38000+38000i$

Algorithms	Errors	Algorithms	Errors
$\alpha = 1$	0	time-dom-algo	0.1081×10^{-14}
fre-dom-algo	0.0352×10^{-14}	$\alpha = 3$	0.0021×10^{-14}
$\alpha = 5$	0.0037×10^{-14}	$\alpha = 7$	0.0051×10^{-14}
$\alpha = 9$	0.0064×10^{-14}	$\alpha = 11$	0.0076×10^{-14}
$\alpha = 13$	0.0089×10^{-14}	$\alpha = 15$	0.0102×10^{-14}
$\alpha = 17$	0.0116×10^{-14}	$\alpha = 19$	0.0131×10^{-14}
$\alpha = 1i$	0.0102×10^{-14}	$\alpha = 3i$	0.0099×10^{-14}
$\alpha = 5i$	0.0125×10^{-14}	$\alpha = 7i$	0.0152×10^{-14}
$\alpha = 9i$	0.0180×10^{-14}	$\alpha = 11i$	0.0207×10^{-14}
$\alpha = 13i$	0.0235×10^{-14}	$\alpha = 15i$	0.0264×10^{-14}
$\alpha = 17i$	0.0293×10^{-14}	$\alpha = 19i$	0.0323×10^{-14}
$\alpha = 1+1i$	0.0215×10^{-14}	$\alpha = 3+3i$	0.0216×10^{-14}
$\alpha = 5+5i$	0.0256×10^{-14}	$\alpha = 7+7i$	0.0301×10^{-14}
$\alpha = 9+9i$	0.0347×10^{-14}	$\alpha = 11+11i$	0.0394×10^{-14}
$\alpha = 13+13i$	0.0442×10^{-14}	$\alpha = 15+15i$	0.0491×10^{-14}
$\alpha = 17+17i$	0.0542×10^{-14}	$\alpha = 19+19i$	0.0593×10^{-14}
$\alpha = 38+38i$	0.1148×10^{-14}	$\alpha = 380+380i$	0.3041×10^{-13}
$\alpha = 3800+3800i$	0.1957×10^{-11}	$\alpha = 38000+38000i$	0.1552×10^{-9}

Table 2

The same with Table 1, but the Morlet wavelet parameters are $\sigma^2 = 1, \eta = 6$

Algorithms	Errors	Algorithms	Errors
$\alpha = 1$	0	time-dom-algo	0.1028×10^{-19}
fre-dom-algo	0.0456×10^{-19}	$\alpha = 3$	0.0027×10^{-19}
$\alpha = 5$	0.0048×10^{-19}	$\alpha = 7$	0.0065×10^{-19}
$\alpha = 9$	0.0081×10^{-19}	$\alpha = 11$	0.0097×10^{-19}
$\alpha = 13$	0.0113×10^{-19}	$\alpha = 15$	0.0130×10^{-19}
$\alpha = 17$	0.0147×10^{-19}	$\alpha = 19$	0.0165×10^{-19}
$\alpha = 1i$	0.0136×10^{-19}	$\alpha = 3i$	0.0132×10^{-19}
$\alpha = 5i$	0.0166×10^{-19}	$\alpha = 7i$	0.0202×10^{-19}
$\alpha = 9i$	0.0239×10^{-19}	$\alpha = 11i$	0.0276×10^{-19}
$\alpha = 13i$	0.0313×10^{-19}	$\alpha = 15i$	0.0351×10^{-19}
$\alpha = 17i$	0.0391×10^{-19}	$\alpha = 19i$	0.0431×10^{-19}
$\alpha = 1+1i$	0.0293×10^{-19}	$\alpha = 3+3i$	0.0293×10^{-19}
$\alpha = 5+5i$	0.0348×10^{-19}	$\alpha = 7+7i$	0.0410×10^{-19}
$\alpha = 9+9i$	0.0473×10^{-19}	$\alpha = 11+11i$	0.0538×10^{-19}
$\alpha = 13+13i$	0.0605×10^{-19}	$\alpha = 15+15i$	0.0674×10^{-19}
$\alpha = 17+17i$	0.0744×10^{-19}	$\alpha = 19+19i$	0.0816×10^{-19}
$\alpha = 38+38i$	0.1598×10^{-19}	$\alpha = 380+380i$	0.4359×10^{-18}
$\alpha = 3800+3800i$	0.2822×10^{-16}	$\alpha = 38000+38000i$	0.2243×10^{-14}

- The running result of GDFT based algorithm is stable and reliable if the absolute value of parameter α is not large enough. For example, for $\alpha = 1, 3, 5, \dots, 19, i, 3i, 5i, \dots, 19i, 1+i, 3+3i, 5+5i, 7+7i$, the errors of GDFT based algorithms are smaller than that of frequency domain algorithm.
- For GDFT based algorithms, if the modulus of the parameter α is too large, the error will increase. For example, the errors of GDFT based algorithm with parameter $\alpha = 38+38i, \alpha = 380+380i, \alpha = 3800+3800i, \alpha = 38000+38000i$ are larger than that of time domain algorithm.

The running time of various algorithms is displayed in Table 3 and Table 4. From Table 3 and Table 4, some information can be drawn.

- GDFT based algorithms run faster than frequency domain algorithm, while frequency domain algorithm runs faster than time domain algorithm [12].
- GDFT based algorithm with parameter 1 or 1i runs faster.

Table 3

The running time of various algorithms, with Morlet wavelet parameters $\sigma^2 = 1$, $\eta = 5$, running 500 times under the same conditions. The unit of running time is second. The various algorithms are time domain algorithm [12, 23], frequency domain algorithm [12, 23], GDFT based algorithm with parameters $\alpha = 1, 3, 5, \dots, 19; i; 3i; 5i, \dots, 19i, 1 + i, 3 + 3i, 5 + 5i, \dots, 19 + 19i, 38 + 38i, 380 + 380i, 3800 + 3800i, 38000 + 38000i$

Algorithms	Time	Algorithms	Time
$\alpha = 1$	0.7349	time-dom-algo	1.8491
fre-dom-algo	1.4809	$\alpha = 3$	1.2911
$\alpha = 5$	1.4006	$\alpha = 7$	1.1428
$\alpha = 9$	1.2184	$\alpha = 11$	1.1773
$\alpha = 13$	1.2366	$\alpha = 15$	1.1947
$\alpha = 17$	1.1478	$\alpha = 19$	1.1621
$\alpha = 1i$	0.8111	$\alpha = 3i$	1.2327
$\alpha = 5i$	1.1755	$\alpha = 7i$	1.1623
$\alpha = 9i$	1.1622	$\alpha = 11i$	1.1641
$\alpha = 13i$	1.1443	$\alpha = 15i$	1.1649
$\alpha = 17i$	1.1602	$\alpha = 19i$	1.1749
$\alpha = 1 + 1i$	1.1113	$\alpha = 3 + 3i$	1.1702
$\alpha = 5 + 5i$	1.1305	$\alpha = 7 + 7i$	1.1430
$\alpha = 9 + 9i$	1.1668	$\alpha = 11 + 11i$	1.1427
$\alpha = 13 + 13i$	1.1444	$\alpha = 15 + 15i$	1.1661
$\alpha = 17 + 17i$	1.1555	$\alpha = 19 + 19i$	1.1426
$\alpha = 38 + 38i$	1.1933	$\alpha = 380 + 380i$	1.1746
$\alpha = (38 + 38i) \times 10^2$	1.1573	$\alpha = (38 + 38i) \times 10^3$	1.1864

Table 4

The same with Table 3, but the Morlet wavelet parameters are $\sigma^2 = 1$, $\eta = 6$

Algorithms	Time	Algorithms	Time
$\alpha = 1$	0.7423	time-dom-algo	1.9305
fre-dom-algo	1.5221	$\alpha = 3$	1.2587
$\alpha = 5$	1.3006	$\alpha = 7$	1.1485
$\alpha = 9$	1.1341	$\alpha = 11$	1.1380
$\alpha = 13$	1.1246	$\alpha = 15$	1.1411
$\alpha = 17$	1.1389	$\alpha = 19$	1.1202
$\alpha = 1i$	0.7973	$\alpha = 3i$	1.2441
$\alpha = 5i$	1.1417	$\alpha = 7i$	1.1332
$\alpha = 9i$	1.1391	$\alpha = 11i$	1.1376
$\alpha = 13i$	1.1665	$\alpha = 15i$	1.1438
$\alpha = 17i$	1.1527	$\alpha = 19i$	1.1714
$\alpha = 1 + 1i$	1.1542	$\alpha = 3 + 3i$	1.1320
$\alpha = 5 + 5i$	1.1246	$\alpha = 7 + 7i$	1.1439
$\alpha = 9 + 9i$	1.1387	$\alpha = 11 + 11i$	1.1221
$\alpha = 13 + 13i$	1.1731	$\alpha = 15 + 15i$	1.1391
$\alpha = 17 + 17i$	1.1540	$\alpha = 19 + 19i$	1.1299
$\alpha = 38 + 38i$	1.1462	$\alpha = 380 + 380i$	1.1584
$\alpha = (38 + 38i) \times 10^2$	1.1507	$\alpha = (38 + 38i) \times 10^3$	1.1854

6. CONCLUSION AND FUTURE WORK

In the generalized Fourier domain based on non causal signals, we prove the time-domain shift property of GDFT. We define the weighted circular convolution of non causal signals and give the relationship between weighted circular convolution and linear convolution. The time invariant property of weighted circular convolution is proposed and proved. Using this property, the computation of CWT is transformed into the computation of weighted circular convolution with any complex parameter a.

Theoretically, GDFT based algorithm with any complex parameter a can be used to calculate CWT. However, if the modulus of the parameter a is too large, the error will increase. We propose the following questions which would be answered in the future.

- How to evaluate the stability and reliability of the algorithm;
- Whether there is some relationship between the error and the modulus of the parameter;
- When the parameter a is in what interval, the result of GDFT based algorithm is stable and reliable.

Therefore, theoretical error analysis [24] is our next research goal.

ACKNOWLEDGEMENTS

The work is supported by the natural science foundation of Jiangxi Province, China (No. 20161BAB201017) and the scientific research foundation of the education bureau of Jiangxi Province, China (No. GJJ201009, No. GJJ170643, No. GJJ190549).

REFERENCES

- [1] N. Holighaus, G. Koliander, Z. Průša, and L.D. Abreu, "Characterization of Analytic Wavelet Transforms and a New Phaseless Reconstruction Algorithm," *IEEE Trans. Signal Process.*, vol. 67, no. 15, pp. 3894–3908, 2019.
- [2] M. Rayeezuddin, B. Krishna Reddy, and D. Sudheer Reddy, "Performance of reconstruction factors for a class of new complex continuous wavelets," *Int. J. Wavelets Multiresolution Inf. Process.*, vol. 19, no. 02, p. 2050067, 2021, doi: [10.1142/S0219691320500678](https://doi.org/10.1142/S0219691320500678).
- [3] Y. Guo, B.-Z. Li, and L.-D. Yang, "Novel fractional wavelet transform: Principles, MRA and application," *Digital Signal Process.*, vol. 110, p. 102937, 2021. [Online]. Available: doi: [10.1016/j.dsp.2020.102937](https://doi.org/10.1016/j.dsp.2020.102937).
- [4] V.K. Patel, S. Singh, and V.K. Singh, "Numerical wavelets scheme to complex partial differential equation arising from Morlet continuous wavelet transform," *Numer. Methods Partial Differ. Equations*, vol. 37, no. 2, pp. 1163–1199, mar 2021.
- [5] C.K. Chui, Q. Jiang, L. Li, and J. Lu, "Signal separation based on adaptive continuous wavelet-like transform and analysis," *Appl. Comput. Harmon. Anal.*, vol. 53, pp. 151–179, 2021.
- [6] O. Erkamaz, I.S. Yapici, and R.U. Arslan, "Effects of obesity on time-frequency components of electroretinogram signal using continuous wavelet transform," *Biomed. Signal Process. Control*, vol. 66, p. 102398, 2021.
- [7] Z. Yan, P. Chao, J. Ma, D. Cheng, and C. Liu, "Discrete convolution wavelet transform of signal and its application on BEV accident data analysis," *Mech. Syst. Signal Process.*, vol. 159, 2021.

- [8] R. Bardenet and A. Hardy, "Time-frequency transforms of white noises and Gaussian analytic functions," *Appl. Comput. Harmon. Anal.*, vol. 50, pp. 73–104, 2021, doi: [10.1016/j.acha.2019.07.003](https://doi.org/10.1016/j.acha.2019.07.003).
- [9] M.X. Cohen, "A better way to define and describe Morlet wavelets for time-frequency analysis," *NeuroImage*, vol. 199, pp. 81–86, 2019, doi: [10.1016/j.neuroimage.2019.05.048](https://doi.org/10.1016/j.neuroimage.2019.05.048).
- [10] H. Yi and H. Shu, "The improvement of the Morlet wavelet for multi-period analysis of climate data," *C.R. Geosci.*, vol. 344, no. 10, pp. 483–497, 2012.
- [11] S.G. Mallat, *A Wavelet Tour of Signal Processing: The Sparse Way*. Academic Press, 2009.
- [12] H. Yi, P. Ouyang, T. Yu, and T. Zhang, "An algorithm for Morlet wavelet transform based on generalized discrete Fourier transform," *Int. J. Wavelets Multiresolution Inf. Process.*, vol. 17, no. 05, p. 1950030, 2019, doi: [10.1142/S0219691319500309](https://doi.org/10.1142/S0219691319500309).
- [13] R. Tolimieri, M. An, and C. Lu, *Algorithms for Discrete Fourier Transform and Convolution*. Springer, 1997.
- [14] J.-M. Attenu and A. Ross, "Method for finding optimal exponential decay coefficient in numerical Laplace transform for application to linear convolution," *Signal Process.*, vol. 130, pp. 47–56, 2017.
- [15] W. Li and A.M. Peterson, "FIR Filtering by the Modified Fermat Number Transform," *IEEE Trans. Acoust. Speech Signal Process.*, vol. 38, no. 9, pp. 1641–1645, 1990.
- [16] M.J. Narasimha, "Linear Convolution Using Skew-Cyclic Convolutions," *Signal Process. Lett.*, vol. 14, no. 3, pp. 173–176, 2007.
- [17] J. Martinez, R. Heusdens, and R.C. Hendriks, "A Generalized Poisson Summation Formula and its Application to Fast Linear Convolution," *IEEE Signal Process Lett.*, vol. 18, no. 9, pp. 501–504, 2011.
- [18] R.C. Guido, F. Pedroso, A. Furlan, R.C. Contreras, L.G. Caobianco, and J.S. Neto, "CWT×DWT×DTWT×SDTWT: Clarifying terminologies and roles of different types of wavelet transforms," *Int. J. Wavelets Multiresolution Inf. Process.*, vol. 18, no. 06, p. 2030001, 2020, doi: [10.1142/S0219691320300017](https://doi.org/10.1142/S0219691320300017).
- [19] P. Kapler, "An application of continuous wavelet transform and wavelet coherence for residential power consumer load profiles analysis," *Bull. Pol. Acad. Sci. Tech. Sci.*, vol. 69, no. 1, p. e136216, 2021, doi: [10.24425/bpasts.2020.136216](https://doi.org/10.24425/bpasts.2020.136216).
- [20] J. Martinez, R. Heusdens, and R.C. Hendriks, "A generalized Fourier domain: Signal processing framework and applications," *Signal Process.*, vol. 93, no. 5, pp. 1259–1267, 2013.
- [21] S. Hui and S.H. Žak, "Discrete Fourier transform and permutations," *Bull. Pol. Acad. Sci. Tech. Sci.*, vol. 67, no. 6, pp. 995–1005, 2019.
- [22] Z. Babic and D.P. Mandic, "A fast algorithm for linear convolution of discrete time signals," in *5th International Conference on Telecommunications in Modern Satellite, Cable and Broadcasting Service. TELSIKS 2001. Proceedings of Papers (Cat. No. 01EX517)*, vol. 2, 2001, pp. 595–598.
- [23] H. Yi, S. Y. Xin, and J. F. Yin, "A Class of Algorithms for ContinuousWavelet Transform Based on the Circulant Matrix," *Algorithms*, vol. 11, no. 3, p. 24, 2018.
- [24] D. Spałek, "Two relations for generalized discrete Fourier transform coefficients," *Bull. Pol. Acad. Sci. Tech. Sci.*, vol. 66, no. 3, pp. 275–281, 2018, doi: [10.24425/123433](https://doi.org/10.24425/123433).